A GENUINELY MULTIDISCIPLINARY JOURNAL

CHEMPLUSCHEM

CENTERING ON CHEMISTRY

Accepted Article

Title: First Family of Amphiphilic Cyclodextrin Liquid Crystals Driven by Dipole-Dipole Interactions

Authors: Chang-Chun Ling; Pier-Luc Champagne; David Ester; Sandra M Ward; Vance E Williams

To be cited as: ChemPlusChem 10.1002/cplu.201600556

Link to VoR: https://doi.org/10.1002/cplu.201600556

A Journal of

ChemPubSoc Europe

WILEY-VCH

www.chempluschem.org

First Family of Amphiphilic Cyclodextrin Liquid Crystals Driven by Dipole-Dipole Interactions

Pier-Luc Champagne,[a] David Ester,[b] Sandra Ward,[c] Vance E. Williams[b] and Chang-Chun Ling*[a]

Abstract: A novel family of amphiphilic cyclodextrin(CD)-based liquid crystals that bear *O*-acetylated oligoethylene glycol chains at the secondary face has been reported. Unlike most of the previously reported liquid crystals based on chemically modified CDs, which depend on H-bonding as the primary intermolecular forces, the present CD derivatives self-assemble into highly ordered smectic liquid crystal phases via the weaker dipole-dipole intermolecular interactions. The obtained materials are found to possess much improved properties such as improved thermostability, reduced clearing temperatures and better fluidity. The present work opens up new possibilities to design CD-based LC materials thus should stimulate future development of LC materials based on CDs.

Introduction

Amphiphilic cyclodextrin (CD) derivatives[1-3] have the ability to self-assemble[4-6] to form ordered superstructures in a solution because of nanosegregation of their polar and apolar groups. In the absence of solvents, amphiphilic CD derivatives can also self-organize through molecular reorganization; new materials such as thermotropic liquid crystals (LCs)[7-10] can be obtained upon changing temperatures. CD-based materials are of particular interest for LC research, because of their relatively rigid, truncated-cone-shaped geometry, making them a unique class of scaffolds. The presence of a hydrophobic cavity in CDs can be further exploited for generating LC materials based on host-guest chemistry.[11] The three common members, α–, β– and γ–CDs, are all polar polyhydroxylated carbohydrates that can be easily turned into amphiphilic materials via installation of aliphatic groups to one of the two ends of the cone.[12-17] The first class of amphiphilic CD derivatives known to form LC mesophases had all primary hydroxyl groups of β–CD replaced with a *n*-octadecylthio group[7] (**1**, Figure **1**), which permits the remaining secondary hydroxyl groups to interact in solid phase, forming a complex network of inter-/intra-molecular H-bonds.[18-19] This H-bond network was believed to be crucial for driving the amphiphilic CDs to self-assemble into thermotropic LCs;[10] it is also the primary intermolecular force used in literature to design amphiphilic CD-based LC mesophases so far.[7-8]

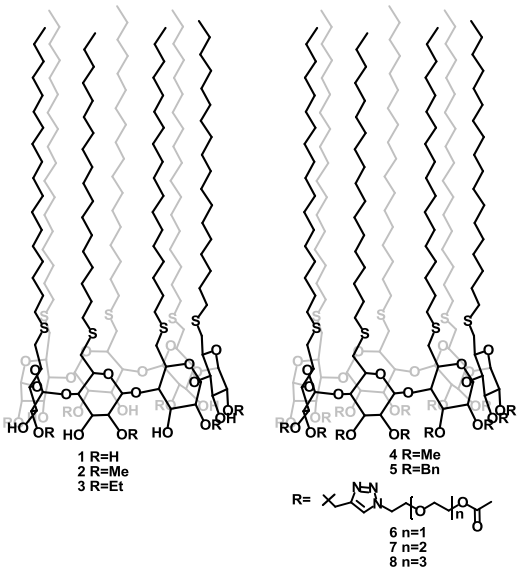

Figure 1. Previously synthesized β-CD derivatives and new targets.

Through a systematic study, previously, we synthesized a series of per-6-*n*-octadecylthio-β-CD derivatives[10] (Figure **1**) that are substituted either at all O-2 positions with an alkyl group of small sizes (such as methyl (**2**), ethyl (**3**) and other lager groups such as allyl and benzyl groups (not shown); it was found only amphiphilic derivatives with smaller alkyl groups (**2**-**3**) formed LC mesophases while the other derivatives with larger substituents did not. We rationalized that the alkyl groups at O-2 positions served the role of delimitating groups that control the distance between secondary face of CD molecules in the bilayers of the solid states, thus they effectively modulate the H-bond strength. Only amphiphilic CD derivatives with smaller groups could form LC mesophases because the molecules of the adjacent layer could get closer, thus interact with each other via a network of intermolecular H-bonds of sufficient strength. On the other hand, when all the secondary hydroxyl groups were substituted with alkyl groups such as methyl (**4**) or benzyl (**5**) groups, they all lost their ability to form H-bond network, thus were unable to form LC mesophases.[10] Although in theory, compound (**5**) could engage a network of π-π interactions between adjacent layers, but clearly, this type of intermolecular force was too weak to induce molecular self-assembling in solid state. In the present work, we report a novel strategy to design CD-based LC materials by

[a] Pier-Luc Champagne, Prof. Dr. Chang-Chun Ling
Alberta Glycomics Centre, Department of Chemistry
University of Calgary
2500 University Drive NW, Calgary Alberta T2N 1N4, Canada
E-mail: ccling@ucalgary.ca
[b] David Ester, Prof. Dr. Vance E. Williams
Department of Chemistry
Simon Fraser University
8888 University Dr, Burnaby, B.C. V5a 1S6 Canada
[c] Prof. Dr. Sandra Ward
Department of Chemistry & Biochemistry
California Polytechnic State University
San Luis Obispo, CA 93407 USA

Supporting information for this article is given via a link at the end of the document.((Please delete this text if not appropriate))

invoking dipole-dipole as the primary intermolecular force to promote self-assembling. We designed a series of *O*-acetylated oligoethylene glycol (OEG) functionalized amphiphilic CD derivatives (**6**-**8**, **Figure 1**) which were synthesized efficiently, and our results revealed that they all possess excellent abilities to form LC mesophases with improved properties. This constitutes the first examples of CD-based LC materials reported in the literatures using dipole-dipole as the principal intermolecular force.

Results and Discussion

Designs and Synthesis

OEGs are polar compounds fully miscible with water because of their multiple polar C-O bonds; the oxygen atoms of OEGs can act as H-bond acceptors and the terminal hydroxyl groups can also act as H-bond donors. This is in contrast with the hydrocarbons which contain only nonpolar C-C and C-H bonds. The difference in polarity prompted us to investigate the possibility of combining both polar OEGs and nonpolar alkyl groups within the CD scaffold; this would create a new class of amphiphilic CD derivatives. Furthermore, if the remaining terminal hydroxyl group of the OEG group is protected, such as with an acetate group, we can prevent the synthesized CD derivatives from interacting with each other via H-bonding in solid phase. Consequently, the strongest intermolecular forces that the targeted CD derivatives could have would be dipole-dipole interactions. Compared to above mentioned CD derivatives, these new CD amphiphiles could have significantly different thermotropic properties in solid states.

Figure 1 shows the design of our synthetic targets **6**-**8** based on β-CD, which have fourteen OEG groups incorporated to the secondary face and seven *n*-octadecyl groups to the primary face. The length of the OEG groups were chosen among those containing 2-4 repeating units of the ethylene glycol, and the involved linking chemistry was the highly efficient copper (I) catalyzed Huisgen 1,3-dipolar cycloaddition.[20-21] We chose to incorporate *n*-octadecylthio groups to the primary face, because previous results showed that this group provided the best LC properties.

Scheme 1 illustrates the synthesis of the key β-CD intermediate **11** that bears fourteen propargyl groups at all O2 and O3 positions and seven mesylates at all the O6 positions. Compound **11** was prepared from the previously reported per-6-*O*-*tert*-butyldimethylsilyl-2,3-di-*O*-propargylated compound **9**[22] which was desilylated with tetra-*n*-butylammonium fluoride in THF as a solvent;[22] we now found the acid (HCl)-catalyzed condition to remove all the *tert*-butyldimethylsilyl groups in a mixture of 2:1 methanol-chloroform[23-24] is more convenient; the desired heptol (**10**) was obtained in 92% yield after a chromatography on silica gel using 15% methanol in dichloromethane as a eluent. The subsequent per-6-mesylation of compound **10** was carried out in anhydrous dichloromethane using methanesulfonyl chloride as a reagent and pyridine as a base to afford the heptamesylate **11** in excellent yield (91%). The 1D ^{1}H NMR spectra of compound **11** showed a singlet at 3.09 ppm which was assigned to be the mesylates, and another two deshielded proton signals at 4.64 and 4.51 ppm, assigned to be the H-6a's and H-6b's of β-CD scaffold, which are significantly deshielded due to the electron-withdrawing effect of the mesylate group. Moreover, another two sets of alkynic protons were observed at 2.55 and 2.53 ppm, respectively, corresponding to the terminal protons of the two types of propargyl groups at the O2- and O3-positions of the CD.

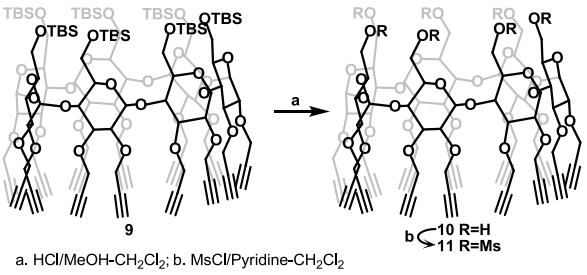

Scheme 1. Preparation of per-6-*O*-mesyl-2,3-*O*-propargylated β-CD intermediate (**11**).

We next undertook the synthesis of three *O*-acetylated OEG reactants **13**, **15** and **19**, containing respectively a di-, tri- and tetra-ethylene glycol unit (**Scheme 2**). Each compound also contained a terminal azido group that can react with the propargyl groups of compound **11**.

As shown in **Scheme 2**, compounds **13**[25] and **15** were prepared respectively from their mono-chlorinated alcohols **12** and **14** in two steps.

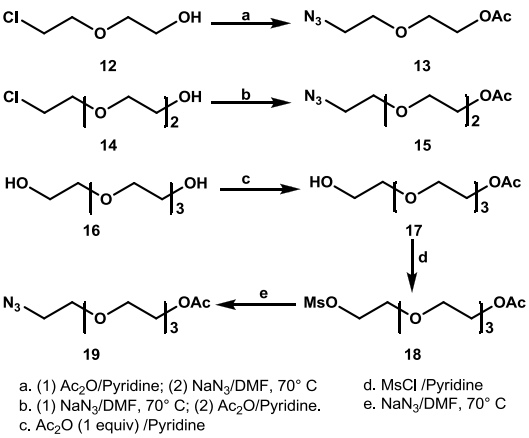

Scheme 2. Preparation of *O*-acetylated di-, tri- and tetra-ethylene glycol azides **15**, **18** and **22** for incorporation to the secondary face of β-CD.

In the case of compound **12**, the terminal hydroxyl group was acetylated first using the conventional acetylation conditions (acetic anhydride/pyridine), and *O*-acetylated intermediates were then subjected to a direct substitution with sodium azide in *N*,*N*-dimethylformamide at 70° C overnight, to afford the desired

compound **13** in 55% combined yield. The preparation of compound **15** was carried out in a similar two-step procedure as **13**, but in reversed order. The combined yield for compound **15** was excellent (91%, two steps).

To synthesize the *O*-acetylated tetraethylene glycol monoazide **19**, we utilized the commercially available alcohol **16** as a starting material. First, a regioselective monoacetylation was carried out using controlled amount of acetic anhydride (1 equiv.) in anhydrous pyridine, this afforded the intermediate mono-ol **17** in 45% yield after a purification by chromatography on silica gel, using a gradient of acetone-toluene as an eluent (10→25%). Compound **17** was then subjected to a mesylation (→**18**, 85% yield) and subsequent azide substitution of the mesylate, affording the desired compound **19** in 86% yield.

With the O_2,O_3-polypropargylated β-CD scaffold **11** and the three *O*-acetylated OEG monoazides **13**, **15** and **19** in hand, we continued our synthesis by preparing the three final targets **6**-**8** (**Scheme 3**). Compound **11** was first coupled with an excess of diethylene glycol azide **13** (1.35 equiv. per C≡CH) via the efficient copper(I)-mediated Huisgen 1,3-dipolar cycloaddition.

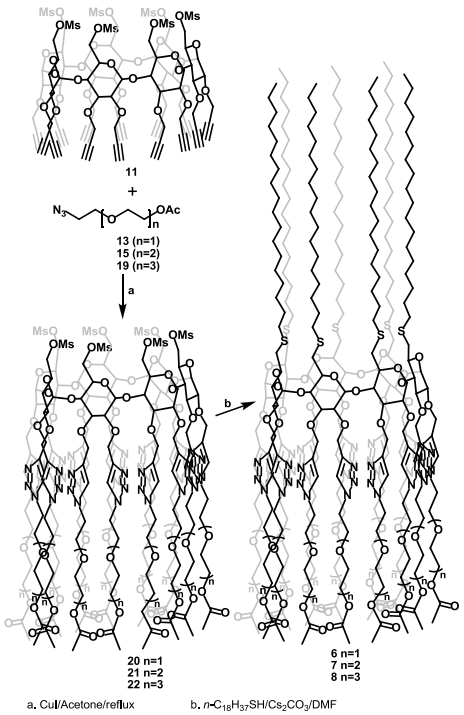

Scheme 3. Cu(I)-mediated Huisgen 1,3-dipolar cycloaddition of *ω*-O-acetylated di- to tetra-ethylene glycol polar residues to the secondary face of β-CD and subsequent n-octadecanethiolation to the primary face.

The reaction was carried out in acetone at 65°C and in the presence of diisopropylethylamine as a base; after stirring for ~20 hours, the desired product **20** that contain seven primary mesylate was isolated in 84% yield by chromatography on silica gel, using a gradient of methanol in dichloromethane (1.5 → 5%) as an eluent.

The completeness of the substitution was confirmed by the presence of a C7 axial symmetry in the ^{1}H NMR spectra of isolated compound **20**. For instance, two sets of triazole protons were observed at 8.06 and 7.94 ppm, each integrated as 7 protons; they correspond to the two groups of triazole fragments attached to the O2 and O3-positions; in addition, the seven mesylates also appeared as a singlet at 3.10 ppm, and the two sets of methylene protons directly attached to O2 and O3 of glucopyranosyl units were observed at 5.19/4.84 ppm and 4.82/4.78 ppm, more deshielded than before, as a result of the formed aromatic 1,2,3-triazole rings. The anomeric protons of all glucopyranosyl units also appeared as a doublet at 5.17 ppm (*J* = 2.9 Hz), while each of the other proton types of the glucopyranosyl units was also observed as a single set of signal with the expected coupling pattern. These are further confirmed by the ^{13}C NMR spectrum (see experimental). Additionally, the identity of compound **20** was also confirmed by the electrospray high-resolution mass spectrometry: expected *m/z*: 2318.7834 for ($C_{175}H_{266}N_{42}O_{91}S_7 + H^+$), found *m/z* 2318.7709.

The two other OEGs conjugates **21** and **22** were also prepared in a similar manner as **20** and the two desired compounds were obtained in pure form in 85% and 76% yields, respectively.

The synthesis of final targets **6-8** required a persubstitution of all 6-mesylates in each of the compounds **20**-**22** with *n*-octadecylthio group. This was carried out in DMF under argon at 75° C using 1-octadecanethiol (5 equiv. per mesylate) as a reagent and cesium carbonate as a base. After stirring overnight, some de-*O*-acetylations were observed, as evidenced by the observation of several closely spaced spots on TLC as well as high resolution mass spectrometry; this was probably due to a nucleophilic attack of *O*-acetates by the octadecylthiolate. Nevertheless, the intermediate products were reacetylated at 65° C using acetic anhydride/pyridine conditions to afford a single spot; after purification by chromatography on silica gel, the target compounds **6, 7** and **8** were isolated in pure form in 63% 97% and 82% yield, respectively.

The structures of all final products were confirmed by ^{1}H and ^{13}C NMR spectra. For example, **Figure 2** shows the ^{1}H-^{13}C HSQC correlation NMR spectrum of compound **6**. As can be seen, the mesylate signals attached to the C-6 were no longer observed (around 3.1 ppm); instead, the two protons (H-6a and H-6b) were then observed at a more shielded region (3.15 ppm and 3.05 ppm), supporting the successful replacement of all mesylates with the less electron withdrawing thiolate, and the two α-methylene protons (adjacent to the sulfur atom) of the octadecylthio groups were observed at 2.58 ppm as a triplet. Finally, a singlet appeared at 2.05 ppm, which corresponded to the two types of acetate groups linked to the end of both O2/O3-OEG chains.

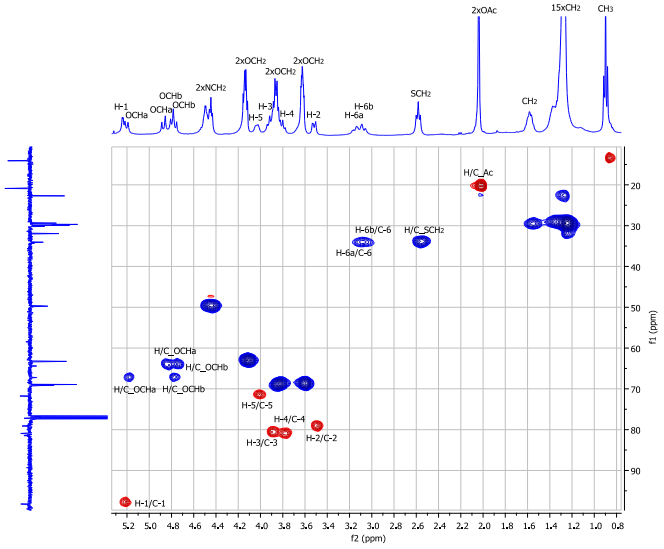

Figure 2. ^{1}H-^{13}C HSQC correlation NMR spectra of compound **6**, recorded in $CHCl_3$ at 400 MHz

The structures of compounds **6**-**8** were further confirmed by high-resolution electrospray ionization mass spectrometry. For example, for compound **6**, a peak at m/z 2984.7654 was observed, which corresponds to the double charged species $[C_{294}H_{504}N_{42}O_{70}S_7 + 2H]^{2+}$ (calc. m/z: 2984.7680). On the other hand, for both compounds **7** and **8**, a peak at m/z 2195.6204 or 2401.0805 was observed in each case, which corresponds respectively to the triple charged species of compound **7** (calculated $[C_{322}H_{560}N_{42}O_{84}S_7 + 3H]^{3+}$: 2195.6368 or compound **8** (calculated $[C_{350}H_{616}N_{42}O_{98}S_7 + 3H]^{3+}$: 2401.0924).

Mesomorphic Properties

All final compounds **6-8** were characterized with thermogravimetric analysis (TGA), Cross-polarized optical microscopy (POM) and differential scanning calorimetry (DSC). TGA revealed both compounds **6** to be stable up to 283 °C (~95%) while compound 7 has similar thermostability - up to 260 °C; the least stable of the three is compound **8** which was found to be stable up to 190 °C (~95%). (See supporting info).

Under POM, the compound with the shortest OEG chains (**6**) cleared at the highest temperature (234.3 °C, Figure **3**a), while increasing the length of the OEG chains had a decreasing effect on their clearing temperature (compound **7**: 194.8 °C; compound **8**: 157.7 °C). This is in sharp contrast with H-bond-mediated LC materials based on CD such as **1**, which was observed to slowly decompose before entering into the isotropic liquid phase.

Upon cooling from their isotropic phases, all three compounds were observed to form LC mesophases. For example, compound **6**, small bâtonnet domains form from the isotropic phase (Figure **3**b); upon further cooling, these domains were observed to grow, and fuse to form larger bâtonnets (Figure **3**c). These bâtonnets are commonly observed at the transition from the isotropic phase to fluid smectic mesophases. This is in contrast with our previously reported H-bond based LC materials of amphiphilic CDs, where the formed mesophases were observed to be much less fluid. Upon further cooling, more organized domains formed and their movement were observed to be gradually reduced and eventually the entire slides were covered with fan-shaped textures as seen in Figure **3**d-e. Compounds **7** and **8** were observed to exhibit similar changes in textures upon cooling as compound **6**, but with phase changes taking place at lower temperature ranges (Figure **3**b-e). Based on the characteristic bâtonnets and fan-shaped textures, compounds **6**-**8** were identified to form smectic A mesophases.

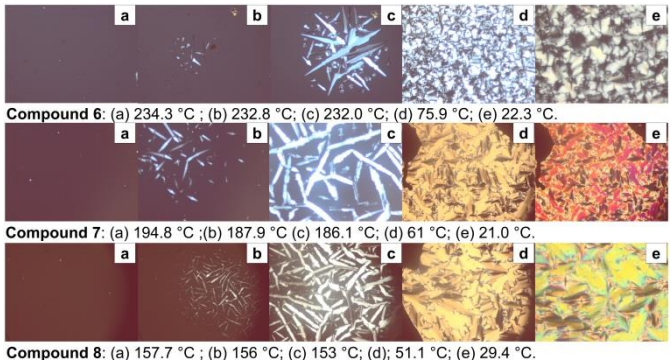

Figure 3. Textures of compounds **6**-**8** observed under POM during cooling from their clearing temperatures. Compound **6** forms a LC phase from ~56 – 230.6 ˚C. Compound **7** forms a LC phase from ~53 – 195. Compound **8** forms a LC phase from ~38 – 159.4.

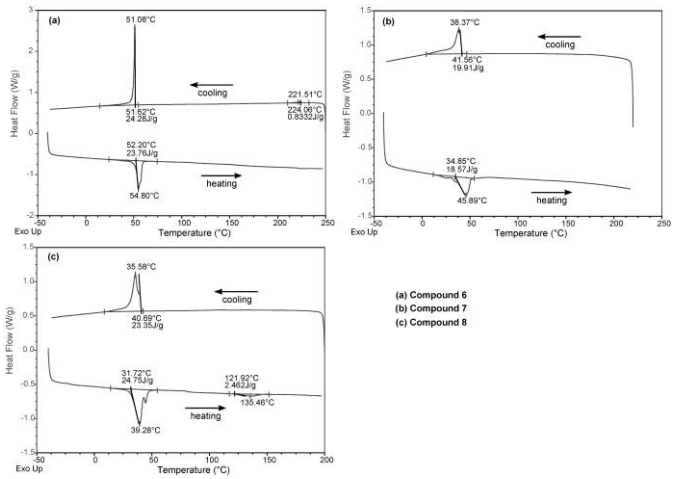

Figure 4. DSC thermograms of compounds **6**-**8**. The first heating cycle for all compounds was omitted because of thermal history.

Figure **4** shows the DSC thermograms obtained for compounds **6**-**8**. As can be seen, all three compounds showed a large endothermic phase transition at the low temperature on heating (54.8 °C for **6**, 45.9 °C for **7** and 39.3 °C for **8**), which was associated with a large enthalpic change (23.8 J/g for **6**, 18.6 J/g for **7** and 39.3 J/g for **8**); these corresponded to the melting of compound **6**-**8** from solid to LC phase in each case.

Each of these transitions was mirrored with a matching large exothermic phase transition (51.1 °C (24.3 J/g) for **6**, 38.4 °C (19.9 J/g) for **7** and 35.6 °C (23.3 J/g) for **8**), which corresponded to the transition of compound **6**-**8** from LC phase to solid phase. However, for all compounds, only small enthalpic changes (< 2.5 J/g) were observed before clearing from LC mesophases into the isotropic phases during the heating cycle, as well as from isotropic phases to LC mesophases during the cooling cycle. Due to a combination of broadening and small enthalpies, some transitions were too broad to be detected by DSC. All these were consistent with Sm A to isotropic phase transitions which are associated with very little change in ordering.

Powder X-Ray Diffraction

Powder X-ray diffraction (XRD) of compound **6** was performed at variable temperatures to confirm the formation of a smectic A LC phases indicated by POM. The diffraction patterns at 20 ˚C and 50 ˚C below the clearing temperature, i.e. ~210 and 180 ˚C respectively, are very consistent. At low angles, we observe sharp (001) and (002) peaks of 48 Å and 24 Å, respectively corresponding to the layered structure of a smectic phase. At higher angles, there is a broad peak at 4.7 Å, indicating a relative lack of order of the molecules within a layer. This XRD data strongly supports the formation of a smectic A LC phase. At room temperature, the X-ray diffraction of this compound shows a similar pattern in the low angle region; with sharp (001), (002), and (003) peaks of 55 Å, 27 Å, and 18 Å, respectively indicating that the lamellar structure is maintained, albeit with an increased layer spacing. In the higher angle region we find that the peak corresponding to a distance of 4.2 Å has grown significantly sharper, consistent with the molecules being much more ordered within the layers. This XRD pattern is consistent with the formation of a higher order smectic phase such as crystal B phase.

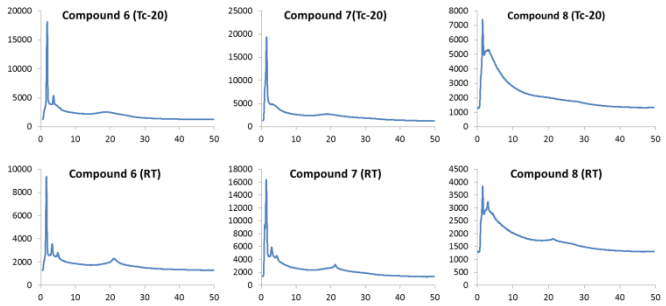

Figure 5. Variable temperature XRD plots of compounds **6**, **7 and 8**, recorded at Tc-20 and room temperature.

For compound **7**, the XRD data obtained was very similar to that of compound **6**, confirming the formation of a smectic A LC phase. The diffraction patterns of the LC phase were also measured at 20 ˚C and 50 ˚C below the clearing temperature. In the low angle region we see a sharp (001) peak corresponding to a layer spacing of 60 Å, as well as a less pronounced (002) peak. At higher angles, a broad peak is observed at 4.6 Å representative of a disordered array of molecules in each layer. This XRD data clearly agrees with the formation of a smectic A LC phase. The room temperature X-ray of this compound was also obtained. Much like compound **6**, the layered structure is maintained; sharp (001), (002), and (003) peaks of 64 Å, 31 Å, and 20 Å respectively are found in the low angle region. Once again, the wide angle peak was observed to grow much sharper at a distance of 4.1 Å indicative of a more ordered array of molecules within the layers.

Similarly, for compound **8**, XRD was measured at 20 ˚C below the clearing temperature (~130 ˚C). In the low angle region, two sharp peaks corresponding to distances 55 Å and 27 Å respectively were observed, which were indexed to the (001) and (002) peaks of a smectic phase. However, no peaks were observed at the high angle region. The absence of peaks at higher angles is not uncommon for the low order smectic phases. The room temperature X-ray of this compound showed that the layered structure was maintained; sharp (001) and (002) peaks associated with a layer spacing of 60 Å are found in the low angle region. Again, no higher angle are peaks observed.

Molecular Packing in Solid State

Molecular modeling showed all compounds **6**-**8** have a conical structure, due to the presence of twice the number of OEG chains at the secondary face than octadecylthio chains on the primary face. In their most extended conformations, the calculated length of compounds **6**, **7** and **8** was about 43.6, 47.7 and 51.4 Å respectively (Figure **6**). Since in all three cases, the X-ray determined periodicity of less than twice the molecular length, this suggests significant intercalation between molecules of adjacent layers. The longest periodicity determined by XRD for compound **8** (55 Å) is unexpectedly shorter than the other two compounds, suggesting slightly increased degrees of intercalation in the LC phase and solid state of this compounds. The wedge shaped geometry of each molecule could be used to explain their smectic packing patterns (Figure **6**). As can be seen, the hydrophobic region is the narrower end of the wedge which is constant for all three compounds, while the hydrophilic OEG chains occupy the wider end of the wedge which increases in length from **6** to **8**. This geometry may lead to a steep increase in curvature of the cone from **6** to **8**. To compensate for this, the hydrophobic tails of compound **8** may intercalate to a greater extent than the others. Additionally, the increasing chain lengths could result in more disorder of the OEG region, leading to them taking up less space vertically and more spaced laterally.

Conclusions

This is the first report of CD-based amphiphilic materials that form LC mesophases via dipole-dipole interactions as the primary intermolecular force. Comparing to the previously reported LC materials based on H-bonding as the primary driving force, the new materials have improved properties, such as lower clearing points, improved molecular stability and improved fluidity. Since the first report of CD-based LC

thermotropic LC more than twenty years ago, there have been only very few examples of CD-based LC materials, the results obtained from current study should stimulate the design and development of future CD-based supramolecular materials by involving other fundamental intermolecular forces.

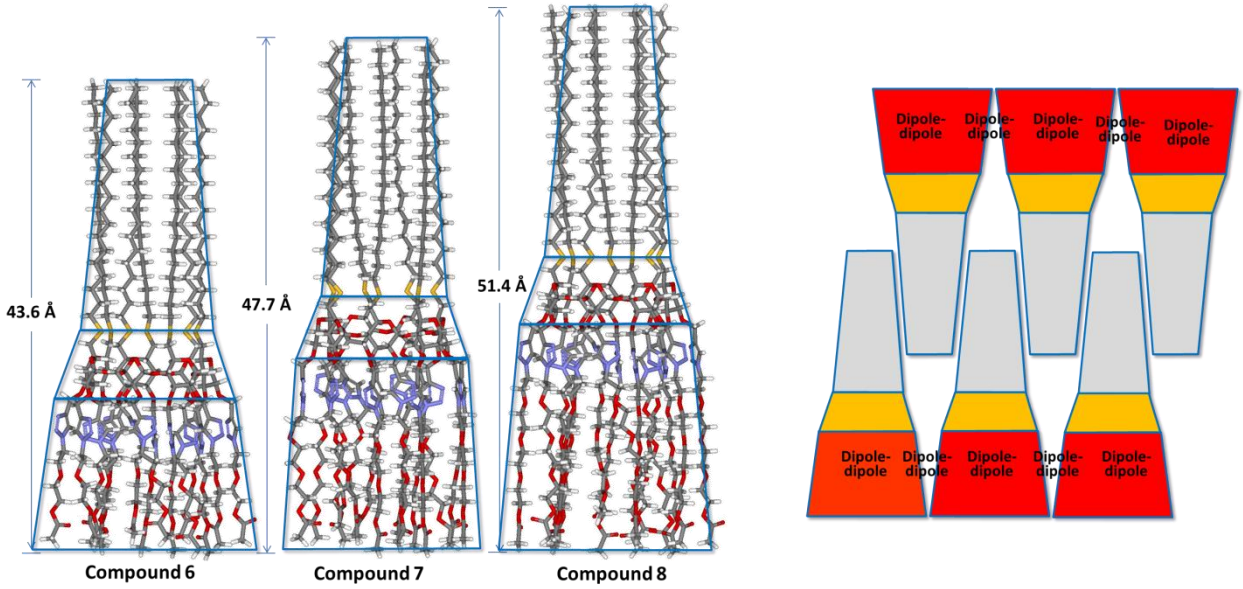

Figure 6. Left: molecular models show compounds **6**, **7** and **8** have respectively a dimension of 43.6, 47.7 and 51.4 Å in the most extended conformation. Right: Proposed bilayer packing of molecules in LC phase and solid state.

Experimental Section

General methods

Analytical TLC was performed on Silica Gel 60-F_{254} (Merck, Darmstadt) with detection by quenching of fluorescence and/or by charring with 5% sulfuric acid in water or with a ceric ammonium molybdate dip. All commercial reagents were used as supplied unless otherwise stated. Column chromatography was performed on Silica Gel 60 (Silicycle, Ontario). Organic solutions from extractions were concentrated under vacuum at < 40 °C (bath). ^{1}H NMR spectra were recorded at 400 MHz on Bruker spectrometers. The first order proton chemical shifts δ_H and δ_C are reported in δ (ppm) and referenced to either residual $CHCl_3$ (δ_H 7.24, δ_C 77.0, $CDCl_3$), residual CD_2HOD (δ_H 3.30, δ_C 49.5, CD_3OD), residual CD_3SOCD_2H (δ_H 2.50, δ_C 39.51, CD_3SOCD_3) or residual C_5D_4HN (δ_H 7.22, δ_C 123.87, C_5D_5N). ^{1}H and ^{13}C NMR spectra were assigned with the assistance of GCOSY, GHSQC spectra. High resolution ESI-QTOF mass spectra were recorded on an Agilent 6520 Accurate Mass Quadrupole Time-of-Flight LC/MS spectrometer. Polarized optical microscopy was performed on OLYMPUS BX-41 equipped with a Linkam hot stage. Thermal analyses were performed using TA-Q200 differential scanning calorimetry instrument. Thermogravimetric Analysis was performed using TGA Q50 instrument.

Per-6-O-*tert*-butyldimethylsilyl-2,3-di-*O*-propargyl–β-cyclodextrin (**9**)

To a solution of per-6-*O*-*tert*-butyldimethylsily-β-CD[26-27] (4.4 g, 2.27 mmol) in anhydrous DMF (40 mL), NaH (60% in mineral oil, 2.55 g, 63.7 mmol, 28 equiv.) was added. The reaction was then cooled to 0˚C, and a solution of 80% propargyl bromide in toluene (14.18 mL, 127 mmol, 56 equiv.) and tetrabutylammonium iodide (TBAI, 260 mg; 0.7 mmol, 0.31 equiv.) was added. After 20 min, MeOH (~ 5 mL) was added to quench the reaction. The solvent was removed under reduced pressure, and the residue was dissolved in ethyl acetate (~ 150 mL). This solution was subsequently washed with water (~ 25 ml), saturated brine solution (2 x 25 mL), and the organic layer was dried over anhydrous Na_2SO_4 and evaporated. The mixture was purified by column chromatography using a mixture of 3% ethyl acetate in hexanes as eluent to afford compound **9** as a colorless foam (3.93 g, 70% yield). R_f = 0.32 (EtOAc: Hexane, 1: 9). ^{1}H NMR (400 MHz, $CDCl_3$) δ 5.23 (d, *J* = 3.5 Hz, 7H, 7 × H-1,), 4.68 (dd, *J* = 15.3, 2.4 Hz, 7H, 7 × H-OC*H*aHb-C≡CH), 4.53 – 4.49 (dd, *J* = 15.3, 2.4 Hz, 7H, 7 × H-OCHa*H*b-C≡CH), 4.52-4.48 (dd, *J* = 16.0, 2.4 Hz, 7H, 7 × H-OC*H*aHb-C≡CH), 4.46-4.42 (dd, *J* = 16.0, 2.4 Hz, 7H, 7 × H-OCHa*H*b-C≡CH), 4.20 – 4.09 (m, 7H, 7 × H-5), 3.90 (dd, *J* = 9.0, 9.0 Hz, 7H, 7 × H-3), 3.84 (dd, *J* = 9.0, 9.0 Hz, 7H, 7 × H-4), 3.66 (dd, *J* = 10.7, ~1 Hz, 7H, 7 × H-6a), 3.59 (dd, *J* = 10.5, ~1 Hz, 7H, 7 × H-6b), 3.50 (dd, *J* = 9.5, 3.5 Hz, 7H, 7 × H-2), 2.53 (dd, *J* = 2.3, 2.3 Hz, 7H, 7 × C≡CH), 2.42 (dd, *J* = 2.3, 2.3 Hz, 7H, 7 × C≡CH), 0.90 (s, 63H, 7 × TBDMS), 0.04 (d, 42H, 7 × TBDMS). *m/z* (HRMS MALDI-TOF) *calcd* for $[C_{1175}H_{336}O_{28}S_7 + Na]^+$ 3133.2805; found: 3133.2754.

Per-2,3-di-*O*-propargyl–β-cyclodextrin (**10**)

Compound **9** (120 mg, 0.049 mmol) was dissolved in a mixture of CH_2Cl_2 – MeOH (2 : 1, 3 mL). After stirring for 5 min, a solution of HCl in MeOH (prepared as previously reported, by adding concentrated HCl to MeOH to obtain pH ~1) was added to the reaction until pH = 1-2, and the progress of the reaction was monitored by TLC using a mixture of 25% ethyl acetate in hexanes and a mixture of 17% MeOH in CH_2Cl_2. Once

the reaction was completed (~2.5 hr), the reaction mixture was concentrated under reduced pressure. The solid residue was purified by column chromatography on silica gel using a 10→15% gradient of MeOH CH_2Cl_2 as eluent to afford the desired compound **10** (74.2 mg, 92%). R_f 0.38 (MeOH : CH_2Cl_2, 20 : 80). ^{1}H NMR (400 MHz, CD_3OD) δ 5.27 (d, *J* = 3.6 Hz, 7H, 7 × H-1), 4.66 (dd, *J* = 15.3, 2.4 Hz, 7H, 7 × OCH*a*-C≡CH), 4.53 (dd, *J* = 15.3, 2.4 Hz, 7H, 7 × OCH*b*-C≡CH), 4.48 (d, *J* =2.4 Hz, 14H, 14 × OCH*a*H*b*-C≡CH), 3.96 (dd, *J* = 12.4, 3.6 Hz, 7H, 7 × H-6a), 3.92 – 3.70 (m, 28H, 7 × H-3, 7 × H-4, 7 × H-6b, 7 x H-5), 3.57 (dd, *J* = 9.4, 3.6 Hz, 7H, 7 x H-2), 2.89 (t, *J* = 2.4 Hz, 7H, 7 × C≡CH), 2.83 (t, *J* = 2.4 Hz, 7H, 7 × C≡CH).

Per-6-*O*-methanesulfonyl-2,3-di-*O*-propargyl-β-cyclodextrin (**11**)

Compound **10** (78 mg, 0.047 mmol) was dissolved in a mixture of anhydrous CH_2Cl_2 (2 mL) and anhydrous pyridine (0.1 mL). The solution was then cooled to 0˚C, and MsCl (0.06 mL, 0.8 mmol, 17.5 equiv.) was then added dropwise. The temperature of the reaction was then allowed to rise gradually to room temperature. After stirring overnight, the mixture was concentrated under reduced pressure. The crude mixture was dissolved in CH_2Cl_2 (~100 mL), and the organic solution was washed with a saturated solution of $NaHCO_3$ (1 x 60mL) and brine (2 x 60 mL), dried over anhydrous Na_2SO_4, evaporated under reduced pressure. The crude product was purified by column chromatography on silica gel using a 10 → 30% gradient of acetone – toluene as the eluent to afford the desired compound **11** (94 mg, 91%). R_f 0.29 (EtOAc : Toluene, 20 : 80). ^{1}H NMR (400 MHz, $CDCl_3$) δ_H 5.28 (d, *J* = 3.7 Hz, 7H, 7 × H-1), 4.64 (dd, *J* = 15.5, 2.4 Hz, 7H, 7 × Ha_Propargyl), 4.62 – 4.55 (m, 14H, 7 × H-6a, 7 × H-6b), 4.52 (dd, *J* = 15.5, 2.4 Hz, 7H, 7 × Hb_Propargyl), 4.48 (overlapped, 7H, 7 × Ha_Propargyl), 4.44 (dd, *J* = 16.4, 2.4 Hz, 7H, 7 × Hb_Propargyl), 3.97 (ddd, *J* = 9.8, 2.9, 2.9 Hz, 7H, 7 × H-5), 3.90 (dd, *J* = 8.8, 9.4 Hz, 7H, 7 × H-4), 3.75 (dd, *J* = 8.9, 9.7 Hz, 7H, 7 × H-3), 3.58 (dd, *J* = 9.7, 3.6 Hz, 7H, 7 × H-2), 3.09 (s, 21H, 7 × OMs), 2.55 (t, *J* = 2.4 Hz, 7H, 7 × C≡CH), 2.53 (dd, *J* = 2.4 Hz, 7H, 7 × C≡CH).

2-(2-Azidoethoxy)ethyl acetate (**13**)

To a solution of 2-(2-Chloroethoxyl)ethanol **12** (2.36 g, 18.9 mmol) in anhydrous pyridine (12 mL), was added acetic anhydride (5.37 mL, 57 mmol, 3 equiv.), and the reaction was stirred overnight. The reaction mixture was concentrated to dryness, and co-evaporated with toluene for several times. The crude intermediate (~2.85 g) was dissolved in DMF (20 mL), and NaN_3 (4.93 g, 75.8 mmol, 4 equiv.) was added. After stirring at 70 ˚C overnight, the mixture was diluted with CH_2Cl_2 (~ 250 mL), washed with saturated brine (3 x 100 mL), the organic solution was subsequently dried over anhydrous Na_2SO_4, and evaporated. The crude mixture was purified by column chromatography on silica gel using a mixture of 10% EtOAc – hexane as eluent to afford the desired compound **13** as a colorless oil (1.82 g, 55% yield). R_f = 0.23 (EtOAc : Hexane, 10 : 90). ^{1}H NMR (400 MHz, $CDCl_3$) 4.24-4.20 (m, 2H, CH_2-OAc), 3.75 (t, *J* = 6.1 Hz, 2H, OCH_2), 3.73-3.69 (m, 2H, OCH_2), 3.62 (t, *J* = 6.1 Hz, 2H, N-CH_2), 2.07 (s, 3H, Ac). ^{13}C NMR (101 MHz, $CDCl_3$) δ 170.86 C=O (OAc), 72.30 (CH_2-OAc), 69.93 (OCH_2), 63.03 (OCH_2), 50.52 N-CH_2, 20.77 (Ac).

2-(2-(2-Azidoethoxy)ethoxy)ethyl acetate (**15**)

To a solution of 2-(2-(2-chloroethoxy)ethoxy)ethanol (**14**, 4.64 g; 27.6 mmol) in anhydrous DMF (20 mL), was added NaN_3 (3.58 g, 55.2 mmol, 2 equiv.), and the mixture was heated to 70 ˚C overnight. The crude mixture was diluted with CH_2Cl_2 (~ 125 mL), washed with saturated brine (2 x 100 mL), dried over anhydrous Na_2SO_4, and evaporated. The crude mixture was purified by column chromatography using a mixture of 15% EtOAc : hexane to afford the monoazide intermediate (~ 4.212 g), which was acetylated using a mixture of pyridine (8 mL) and acetic anhydride (4.55 mL, 48 mmol) at 70 ˚C. After stirring for 7 hrs, the mixture was evaporated to dryness under reduced pressure. The mixture was purified by column chromatography on silica gel using a 5 → 10% gradient of EtOAc - hexane) as the eluent to afford the desired compound **15** (5.01 g, 91% over 2 steps). R_f 0.20 (EtOAc : Hexane, 20:80). ^{1}H NMR (400 MHz, $CDCl_3$) δ 4.18-4.13 (m, 2H, CH_2-OAc), 3.68-3.64 (m, 2H, OCH_2-c), 3.64-3.61 (m, 2H, OCH_2-d), 3.61-3.58 (m, 4H, 1 X OCH_2-b, 1 X OCH_2-e), 3.32 (t, *J* = 5.2 Hz, 2H, N-CH_2), 2.01 (s, 3H, Ac). ^{13}C NMR (101 MHz, $CDCl_3$) δ 170.86 C=O (OAc), 71.32 (CH_2-OAc), 70.59 (OCH_2), 70.54 (OCH_2), 70.01 (OCH_2), 63.47 (N_3-CH_2-CH_2), 50.60 (N_3-CH_2), 20.81 (Ac).

2-(2-(2-(2-Hydroxyethoxy)ethoxy)ethoxy)ethyl acetate (**17**)

A solution of tetraethyleneglycol (**16**, 2.25 g; 12 mmol) in anhydrous pyridine (6 mL) and acetic anhydride (1.1 mL, 11.6 mmol) was stirred at room temperature overnight. The mixture was concentrated under reduced pressure and co-evaporated with toluene. The crude mixture was purified by column chromatography on silica gel using a 10 → 25% gradient of acetone – toluene as the eluent to afford the desired product **17** as a colorless oil (1.84 g, 67%). R_f 0.57 (acetone : toluene, 60:40). ^{1}H NMR (400 MHz, $CDCl_3$) δ 4.20 (t, *J* = 4.8 Hz, 2H, CH_2-OAc), 3.70 – 3.63 (m, 12H, 6 x CH_2), 3.60 – 3.57 (m, 2H, CH_2-OH), 2.71 (s, 1H, OH), 2.05 (s, 3H, OAc).

2-(2-(2-(2-Azidoethoxy)ethoxy)ethoxy)ethyl acetate (**19**)

Compound **17** (1.84 g, 0.008 mol) was dissolved in anhydrous CH_2Cl_2 (4 mL) and pyridine (0.02 mol, 1.89 mL); the reaction mixture was cooled to 0˚C, and MsCl (1.21 mL, 0.016 mol, 2 equiv.) was added dropwise. After stirring overnight, the reaction mixture was concentrated under reduced pressure, and the residue was purified by column chromatography on silica gel using 3% MeOH – CH_2Cl_2 as the eluent to afford the desired product (**18**) as a colorless oil (1.98 g, 81%), which was used directly for the next step.

To a solution of compound **18** (2.98 g, 9.5 mmol) in DMF (5 mL), was added NaN_3 (1.23 g, 18.9 mmol, 2.0 equiv.), and the reaction was stirred at 70˚C overnight. The reaction mixture was concentrated under reduced pressure. The crude mixture was worked up as above and purified by column chromatography on silica gel using a 10 → 15% gradient of acetone – hexane as the eluent. The desired product **19** (2.13 g) was isolated as a colorless oil in 86% yield. R_f 0.49 (Acetone : Hexane, 30:70). ^{1}H NMR (400 MHz, $CDCl_3$) δ_H 4.14 (t, *J* = 4.8 Hz, 2H, CH_2-OAc), 3.64-3.57 (m, 12H, 6 × OCH_2), 3.31 (t, *J* = 5.1 Hz, 2H, N-CH_2), 2.00 (s, 3H, Ac). ^{13}C NMR (101 MHz, $CDCl_3$) δ 170.74 C=O (OAc), 70.89-70.27 (OCH_2), 69.82 (OCH_2), 68.88 (OCH_2), 63.39 (N_3-CH_2-CH_2), 50.48 (N_3-CH_2), 20.62 (Ac).

Compound (**20**)

To a solution of heptamesylate **11** (120 mg; 0.05 mmol) in acetone (2.5 mL), was added monoazide **13** (0.197 g, 1.1 mmol, 21 equiv.) DIPEA (20 µL, 0.015 mmol; 0.3 equiv.) and CuI (20 mg, 0.11mmol, 0.14 eq); the reaction was heated to 65 ˚C under argon overnight. More monoazide **13** (0.09 g, 0.5 mmol, 9.8 equiv.), DIPEA (20 µL, 0.015 mmol, 0.3 eq) and CuI (20 mg, 0.1 mmol, 0.002eq) were added, and the reaction was continued for another 6 hrs under at the same temperature. The reaction mixture was concentrated under reduced pressure. The solid residue was partitioned between ethyl acetate (125 mL) and 10% aqueous EDTA (2 x 50 mL) solution for 30 min. The organic layer was separated, dried over anhydrous Na_2SO_4 and evaporated. The crude mixture was purified

by column chromatography on silica gel using a 1.5 → 5% gradient of MeOH – CH_2Cl_2 as the eluent. The desired product **20** was isolated as a white foam (211 mg, 84% yield). R_f 0.35 (MeOH : CH_2Cl_2, 5 : 95). $[\alpha]_D$= 14.23 (*c* 5.2, CH_2Cl_2). ^{1}H NMR (400 MHz, $CDCl_3$) δ_H 8.06 (s, 7H, 7 × H triazole), 7.94 (s, 7H, 7 × H triazole), 5.22-5.13 (m, 14H, 7 × OCHaHb-triazole, 7 × H-1), 4.91-4.73 (m, 21H, 21 × OCHaHb-triazole), 4.64 – 4.57 (m, 14H, 7 × H-6a, 7 × H-6b), 4.54 (t, *J* = 5.0 Hz, 14H, 7 × N-CH_2), 4.48 (t, *J* = 5.4 Hz, 14H, 7 × N-CH_2), 4.19-4.11 (m, 28H, 14 × CH_2-OAc), 4.06 – 3.94 (m, 14H, 7 × H-5, 7 × H-3), 3.91 (t, *J* = 5.2 Hz, 14H, 7 × CH_2-b), 3.85 (t, *J* = 5.1 Hz, 14H, 7 × CH_2-b), 3.71 – 3.56 (m, 35H, 7 × H-4, 28 × OCH_2), 3.54 (dd, *J* = 9.5, 2.5 Hz, 7H, 7 × H-2), 3.10 (s, 21H, 7 × Ms), 2.04 (s, 42H, 14 × OAc). ^{13}C NMR (100 MHz, $CDCl_3$) δc 170.93 (x 14, C=O), 145.10 (x 7, triazole), 144.21 (x 7, triazole), 124.81 (x 7, triazole), 124.43 (x 7, triazole), 98.65 (x 7, C-1), 80.58 (x 7, C-3), 78.91 (x 7, C-4), 78.27 (x 7, C-2), 70.37 (x 21, OCH_2), 69.52 (x 7, C-5), 69.23 (x 7, CH_2-b1), 69.16 (x 7, CH_2-b2), 68.95 (x 35, OCH_2, N-CH_2-b, C-6), 67.73 (x 7, CH_2-triazole), 64.39 (x 7, CH_2-triazole), 63.23 (x 14, CH_2-OAc), 49.89 (x 7, N-CH_2), 49.78 (x 7, N-CH_2), 37.21 (x 7, Mes), 20.82 (x 14, OAc). *m/z* (HRMS MALDI-TOF) calcd for $[C_{175}H_{266}N_{42}O_{91}S_7 + 2H]^{2+}$: 2318.7834, found: 2318.7709.

Compound (**21**)

Compound **21** was obtained similarly as **20** using heptamesylate **11** (120 mg; 0.05 mmol), monoazide **15** (0.27 g 1.26 mmol), DIPEA (20 µL, 1.9 mmol), CuI (20 mg) at 65 ˚C. The pure product **21** (265 mg, 0.050 mmol) was isolated in 93% yield by column chromatography on silica gel using a 3 → 6% gradient of MeOH – CH_2Cl_2 as the eluent. R_f 0.35 (MeOH : CH_2Cl_2, 10 : 90). $[\alpha]_D$ = 17.95 (*c* 3.9, CH_2Cl_2). ^{1}H NMR (400 MHz, $CDCl_3$) δ 8.05 (s, 7H, 7 × H triazole), 7.93 (s, 7H, 7 × H triazole), 5.19 (d, *J* = 11.4 Hz, 7H, 7 × OCHaHb-triazole), 5.15 (d, *J* = 3.4 Hz, 7H, 7 × H-1), 4.88-4.74 (m, 21H, 21 × OCHaHb-triazole), 4.62 – 4.56 (m, 14H, 7 × H-6a, 7 x H-6b), 4.54 (t, *J* = 5.6 Hz, 14H, 7 × N-CH_2), 4.48 (t, *J* = 5.4 Hz, 14H, 7 × N-CH_2), 4.23-4.16 (m, 28H, 14 × CH_2-OAc), 4.04 – 3.98 (m, 7H, 7 × H-5), 3.98 – 3.94 (m, 7H, 7 × H-3), 3.91 (t, *J* = 5.7 Hz, 14H, 7 × CH_2-b), 3.86 (t, *J* = 5.4 Hz, 14H, 7 × CH_2-b), 3.71 – 3.56 (m, 91H, 7 x H-4, 14 x CH_2-c, 14 × CH_2-d, 14 × CH_2-e), 3.54 (dd, *J* = 9.7, 3.4 Hz, 7H, 7 × H-2), 3.09 (s, 21H, 7 × Ms), 2.07 (s, 42H, 14 × OAc). ^{13}C NMR (100 MHz, $CDCl_3$) δc 170.93 (14 x C=O), 145.11 (7 x C-quaternary-triazol), 144.22 (7 x C-quaternary-triazole), 124.79 (7 x CH-triazol), 124.44 (7 x CH-triazol), 98.65 (7 x C-1), 80.58 (7 x C-3), 78.91 (7 x C-4), 78.27 (7 x C-2), 70.37 (21 x OCH_2), 69.58 (7 x C-5), 69.05 (21 x OCH_2, 14 x N-CH_2-b, 7 x C-6), 67.30 (7 x CH_2-beside-triazole), 64.30 (7 x CH_2-beside-triazole), 63.49 (14 x CH_2-OAc), 49,96 (7 x N-CH_2), 49.83(7 x N-CH_2), 37.13(7 x Mes), 20.63(14 x CH_3(OAc)). *m/z* (HRMS MALDI-TOF) calcd for $[C_{203}H_{322}N_{42}O_{105}S_7 + 3H]^{3+}$: 1751.6470, found: 1751.6397.

Compound (**22**)

Compound **22** was obtained similarly as **20** using heptamesylate **11** (96 mg; 0.04 mmol), monoazide **19** (0.32 g 1.9 mmol), DIPEA (20 µL, 1.9 mmol), CuI (20 mg, 0.11 mmol, 0.17 equiv.) at 55 ˚C. The pure product **22** (194 mg, 0.033 mmol) was isolated in 76% yield by column chromatography on silica gel using a 2 → 5% gradient of MeOH – CH_2Cl_2 as the eluent. R_f 0.3 (MeOH: CH_2Cl_2, 5: 95). $[\alpha]_D$ = 12.0 (*c* 9, CH_2Cl_2). ^{1}H NMR (400 MHz, $CDCl_3$): δ_H 8.05 (s, 7H, 7 × H_triazole), 7.91 (s, 7H, 7 × H_triazole), 5.18 (d, *J* = 11.0 Hz, 7H, 7 × OC*H*aHb-triazole), 5.13 (d, *J* = 2.9 Hz, 7H, 7 × H-1), 4.83 (m, 14H, 14 × OC*HaH*b-triazole), 4.76 (d, *J* = 12.7 Hz, 7H, 7 × OCHa*H*b-triazole) 4.62 – 4.55 (m, 14H, 7 × H-6a, 7 × H-6b), 4.53 (t, *J* = 5.4 Hz, 14H, 7 × N-CH_2), 4.47 (t, *J* = 5.3 Hz, 14H, 7 × N-CH_2), 4.24 - 4.19 (m, 28H, 14 × CH_2-OAc), 4.06 – 3.95 (m, 7 × H-5, 7H), 3.96 – 3.89 (m, 21H, 7 × H-3, 7 × OCH_2), 3.86 (t, *J* = 5.4 Hz, 21H, 7 × OCH_2), 3.71 – 3.56 (m, 147H, 7 × H-4, 70 x OCH_2), 3.53 (dd, *J* = 9.7, 2.9 Hz, 7H, 7 × H-2), 3.09 (s, 21H, 7 × Ms), 2.07 (s, 42H, 14 × OAc). ^{13}C NMR (100 MHz, $CDCl_3$) δc 171.0 (x 14, C=O), 145.1 (x 7, triazole), 144.2 (x 7, triazole), 124.8 (x 7, triazole), 124.4 (x 7, triazole), 98.7 (x 7, C-1), 80.6 (x 7, C-3), 78.9 (x 7, C-4), 78.2 (x 7, C-2), 70.5-70.3 (x 28, OCH_2), 69.6 (x 7, C-5), 69.1-69.4 (x 49, OCH_2, N-CH_2-b, C-6), 67.2 (x 7, CH_2-triazole), 64.3 (x 7, CH_2-triazole), 63.5 (x 14, CH_2-OAc), 49.9 (x 7, N-CH_2), 49.8 (x 7, N-CH_2), 37.1 (x 7, Ms), 21.0 (x 14, OAc). *m/z* (HRMS MALDI-TOF) calcd for $[C_{231}H_{378}N_{42}O_{119}S_7 + 2H]^{2+}$: 2935.1504, found: 2935.1303.

Compound (**6**)

Compound **20** (12 mg, 0.003 mmol) was dissolved DMF (0.5 mL) under argon. To this solution, was added Cs_2CO_3 (24 mg, 0.073 mmol), *n*-$C_{18}H_{37}SH$ (26 mg, 0.091 mmol); the mixture was then heated overnight at 75 ˚C. The reaction mixture was then evaporated to dryness under reduced pressure. The residue was dissolved in CH_2Cl_2, and filtered off by column chromatography on silica gel using 5% MeOH - CH_2Cl_2 as the eluent. The fractions containing partially de-*O*-acetylated products (charred with 5% H_2SO4 on TLC) were pooled and evaporated to dryness. The mixture was reacetylated using a mixture of pyridine (0.6 mL) and acetic anhydride (0.5 mL) at 60˚C for 1 hour. The reaction mixture was evaporated to dryness under reduced pressure again. The residue was purified by column chromatography on silica gel using a 3 → 5% gradient of MeOH – CH_2Cl_2 as the eluent to afford the pure product **6** (12 mg, 77% yield) as a clear wax. R_f 0.37 (MeOH : CH_2Cl_2, 6 : 94). $[\alpha]_D$ 18 (*c* 8.0, CH_2Cl_2). ^{1}H NMR (400 MHz, $CDCl_3$) δ_H 8.02 (s, 7H, 7 × H_triazole), 7.98 (s, 7H, 7 × H_triazole), 5.24 (d, *J* = 2.9 Hz, 7H, 7 × H-1), 5.20 (d, *J* = 11.0 Hz, 7H, 7 × OC*H*aHb-triazole), 4.87 (d, *J* = 12.4 Hz, 7H, 7 × OC*H*aHb-triazole) 4.80 (d, *J* = 10.7 Hz, 7H, 7 × OCHa*H*b-triazole), 4.77 (d, *J* =12.0 Hz, 7H, 7 × OCHa*H*b-triazole) 4.56 – 4.47 (m, 14H, 7 × N-CH_2), 4.45 (t, *J* = 5.4 Hz, 14H, 7 × N-CH_2), 4.21-4.10 (m, 28H, 14 × C*H*$_2$-OAc), 4.06 – 4.00 (m, 7H, 7 × H-5), 3.97 - 3.75 (m, 42H, 14 × OCH_2, 7 × H-3, 7 × H-4), 3.69 – 3.56 (m, 28H, 14 × OCH_2), 3.52 (m, 7H, 7 × H-2), 3.23-3.00 (m, 14H, 7 × H-6a, 7 × H-6b), 2.58 (t, *J* = 7.4 Hz, 14H, 7 × S-CH_2_octadecyl), 2.04 (s, 42H, 14 × OAc), 1.58 (m, 14H, 7 × SCH$_2$C*H*$_2$_octadecyl), 1.32-1.25 (m, 210H, 105 × CH_2_octadecyl), 0.90 (t, *J* = 6.9 Hz, 21H, 7 × CH_3_octadecyl). ^{13}C NMR (100 MHz, $CDCl_3$) δ_C 170.79 (C=O), 145.10 (triazole), 145.32 (triazole), 144.75 (triazole), 124.86 (triazole), 124.42 (triazole), 98.25 (C-1), 81.46 (C-4), 80.92 (C-3), 78.27 (C-2), 71.76 (C-5), 69.18 (OCH_2), 69.14 (OCH_2), 68.92 (O-CH_2), 67.32 (OCH_2-triazole), 64.35 (OCH_2-triazole), 63.23 (*C*H$_2$-OAc), 49.75 (N-CH_2), 49.65 (N-CH_2), 34.33 (C-6), 34.07 (S-CH_2), 29.32-31.98 (CH_2_octadecyl), 22.29 (CH_2_octadecyl), 20.85 (OAc), 14.10 (CH_3_octadecyl). *m/z* (HRMS MALDI-TOF) calcd for $[C_{294}H_{504}N_{42}O_{70}S_7 + 2H]^{2+}$: 2984.7680, found: 2984.7654.

Compound (**7**)

Compound **21** (47 mg; 0.009 mmol) was reacted with Cs_2CO_3 (61 mg, 0.19 mmol), n-$C_{18}H_{37}SH$ (17 mg, 0.058 mmol) in a mixture of DMF (0.25 mL) and THF (0.25 mL) as compound **6**. The partially O-deacetylated intermediates were isolated and reacetylated as above using pyridine (0.6 mL) and Ac_2O (0.5 mL) at 60˚C for 1 hr and after evaporation, the reaction mixture was purified by column chromatography on silica gel using a 3 → 5% gradient of MeOH – CH_2Cl_2 as the eluent. The pure product **7** (57.2 mg) was isolated as a clear wax in 97% yield. R_f 0.42 (MeOH : CH_2Cl_2, 8 : 92). $[\alpha]_D$ = 13.6 (*c* 2.4, CH_2Cl_2). ^{1}H NMR (400 MHz, $CDCl_3$): δ 8.02 (s, 7H, 7 × H_triazole), 7.99 (s, 7H, 7 × H_triazole), 5.31-5.10 (m, 14H, 7 × H-1, 7 × OC*H*aHb-triazole), 4.87 (d, *J* = 12.4 Hz, 7H, 7 × OC*H*aHb-triazole) 4.80 (d, *J* = 10.7 Hz, 7H, 7 × OCHa*H*b-triazole), 4.92 - 4.73 (m, 21H, 21 × OCHaHb-triazole) 4.57– 4.48 (m, 14H, 7 × N-CH_2), 4.45 (t, *J* = 5.3 Hz, 14H, 7 × N-CH_2), 4.22 - 4.16 (m, 28H, 14 × CH_2-OAc), 4.06 – 4.00 (m, 7H, 7 × H-5), 3.96 - 3.91 (m, 7H, 7 × H-3), 3.91 - 3.83 (m, 28H, 14 × OCH_2), 3.78 (dd, *J* = 8.8, 8.8 Hz, 7H, 7 × H-4), 3.69 – 3.62 (m,

28H, 14 × OCH_2), 3.62 - 3.54 (m, 28H, 28 × OCH_2), 3.52 (dd, *J* = 9.6, 3.1 Hz, 7H, 7 × H-2), 3.22 - 2.97 (m, 14H, 7 × H-6a, 7 × H-6b), 2.58 (t, *J* = 7.3 Hz, 14H, 7 × S-CH_2_octadecyl), 2.07 (s, 42H, 14 × OAc), 1.62 - 1.52 (m, 14H, 7 × SCH_2CH_2_octadecyl), 1.32 - 1.25 (m, 210H, 105 × CH_2_octadecyl), 0.94 (t, *J* = 6.7 Hz, 21H, 7 × CH_3_octadecyl). ^{13}C NMR (100 MHz, $CDCl_3$): δ_C 170.9 (C=O), 145.3 (triazole), 144.7 (triazole), 124.8 (triazole), 124.4 (triazole), 98.3 (C-1), 81.5 (C-4), 81.0 (C-3), 79.0 (C-2), 71.7 (C-5), 70.3 - 70.5 (OCH_2), 69.4 (OCH_2), 69.3 (OCH_2), 69.1 (OCH_2), 69.1 (N-CH_2), 67.2 (OCH_2-triazole), 64.3 (OCH_2-triazole), 63.2 (CH_2-OAc), 49.9 (N-CH_2), 49.8 (N-CH_2), 34.3 (C-6), 34.1 (S-CH_2), 29.3 - 31.9 (CH_2_octadecyl), 22.7 (CH_2_octadecyl), 20.9 (OAc), 14.1 (CH_3_octadecyl). *m/z* (HRMS MALDI-TOF) calcd for $[C_{322}H_{560}N_{42}O_{84}S_7 + 3H]^{3+}$ calc.: 2195.6368, found: 2195.6204.

Compound (**8**)

Compound **8** was prepared from compound **22** (16 mg; 0.0027 mmol) Cs_2CO_3 (12.4 mg, 0.04 mmol;), n-$C_{18}H_{37}SH$ (11 mg, 0.040 mmol) in DMF (1.5 mL) at 60 ˚C as compound **6**. The partially O-deacetylated intermediates were isolated by column chromatography (1 → 5% MeOH – CH_2Cl_2) and reacetylated at 60 ˚C for 1 hr using a mixture of pyridine (0.6 mL) and acetic anhydride (0.5 mL) as above. The pure product **8** (15.8 mg) was isolated as a clear wax in 82% yield by column chromatography using a 1 → 5% gradient. R_f 0.42 (MeOH : CH_2Cl_2, 8 : 92). $[\alpha]_D$ +26.4 (*c* 2.4, CH_2Cl_2). ^{1}H NMR (400 MHz, $CDCl_3$): δ_H 8.01 (s, 7H, 7 × H_triazole), 8.00 (s, 7H, 7 × H_triazole), 5.23 (d, *J* = 9.6 Hz, 7H, 7 × OC*H*aHb-triazole), 5.13 (d, *J* = 2.6 Hz, 7H, 7 × H-1), 4.89 - 4.73 (m, 21H, 7 × OC*H*aHb-triazole, 14 × OCHa*H*b-triazole), 4.51 (t, *J* = 5.5 Hz, 14H, 7 × N-CH_2), 4.45 (t, *J* = 5.5 Hz, 14H, 7 × N-CH_2), 4.24 - 4.20 (m, 28H, 14 × CH_2-OAc), 4.05 – 3.99 (m, 7H, 7 × H-5), 3.94 – 3.84 (m, 35H, 7 × H-3, 14 × OCH_2), 3.77 (dd, *J* = 8.6, 8.6 Hz, 7H, 7 × H-4), 3.71 – 3.67 (m, 28H, 14 × OCH_2), 3.66 - 3.54 (m, 112H, 56 × OCH_2), 3.52 (dd, *J* = 9.7, 3.0 Hz, 7H, 7 × H-2), 3.14 (dd, *J* = 12.4, <1 Hz, 7H, 7 × H-6a), 3.07 (dd, *J* = 12.5, <1 Hz, 7H, 7 × H-6b), 3.09 (s, 21H, 7 × OMs), 2.57 (t, *J* = 7.4 Hz, 14H, 7 × S-CH_2_octadecyl), 2.08 (s, 42H, 14 × OAc), 1.58 (m, 14H, 7 × SCH_2CH_2_octadecyl), 1.33 - 1.24 (m, 210H, 105 × CH_2_octadecyl), 0.90 (t, *J* = 6.7 Hz, 21H, 7 × CH_3_octadecyl). ^{13}C NMR (100 MHz, $CDCl_3$): δ_C 170.9 (C=O), 145.2 (triazole), 144.6 (triazole), 124.8 (triazole), 124.4 (triazole), 98.3 (C-1), 81.5 (C-4), 80.9 (C-3), 79.0 (C-2), 71.7 (C-5), 70.5 (OCH_2), 70.4 (OCH_2), 70.4 (OCH_2), 69.4 (OCH_2), 69.3 (OCH_2), 69.1 (N-CH_2), 67.2 (OCH_2-triazole), 64.2 (OCH_2-triazole), 63.6 (CH_2OAc), 49.9 (N-CH_2), 49.8 (N-CH_2), 34.3 (C-6), 34.1 (S-CH_2_octadecyl), 29.19 - 31.93 (CH_2_octadecyl), 22.7 (CH_2_octadecyl), 20.9 (OAc), 14.1 (CH_3_octadecyl). *m/z* (HRMS MALDI-TOF) calcd for $[C_{350}H_{616}N_{42}O_{98}S_7 + 3H]^{3+}$ calc.: 2401.0924, found: 2401.0805.

Powdered X-ray crystallography

Samples were heated to the isotropic liquid phase on a hot plate and loaded by capillary action. Excess material was cleaned off the sides with clean dry tweezers. Capillaries were then cut to length and mounted in a capillary furnace.[28] Measurements were carried out on a Rigaku RAXIS rapid diffractometer using Cu Ka radiation (λ=1.5418 Å), a graphite monochromator and a Fujifilm Co. Ltd curved image plate (460 mm x 256 mm). Temperature was controlled with an Omega temperature controller connected to the capillary furnace with a K-type thermocouple for feedback. Owing to technical issues, the controller was set to manual mode. Due to thermal equilibration, the temperature often dropped during the course of acquisition. Only the final temperature is reported. A 0.3 mm collimator was used and all samples were irradiated for 30 minutes. Peaks and their respective angle measurements and d-spacings were determined using the MDL JADE software. Peak type was analysed by taking the reciprocal d-spacings and dividing them by the highest intensity peak, unless otherwise noted. Only peaks with greater than 1% intensity in the low angle region were analysed.

Molecular Modelling

The three dimensional coordinates of the β-CD scaffold were taken from its crystal structure[29] and modified using Insight II/Builder module to obtain the molecular model of compounds **6**-**8**. The atomic potentials and partial charges of the three molecules were assigned using the CVFF forcefield and their geometries were subsequently minimized within Insight II/Discover module using the Steepest Descent algorithm (maximum RMS derivative = 0.1 kcal/Å; ε=1).

Acknowledgements

We are grateful to Dr. Ping Zhang for recording all the HRMS of compounds reported in this work and for her insightful advice, to Dr. Thomas Baumgartner for the use of the TGA Q50 thermogravimetric analysis instrument. The financial support from Alberta Innovates – Technology Futures, the Natural Sciences and Engineering Research Council of Canada, and the University of Calgary are greatly acknowledged.

Keywords: Cyclodextrin • Liquid Crystal • Dipole-dipole interactions • Supramolecular self-assembly • Oligoethylene glycol

[1] E. Bilensoy, A. A. Hincal, *Expert Opin. Drug Deliv.* **2009**, *6*, 1161–1173.
[2] F. Sallas, R. Darcy, *Eur. J. Org. Chem.* **2008**, 957–969.
[3] A. Méndez-Ardoy, M. Gómez-García, C. O. Mellet, N. Sevillano, M. Dolores Girón, R. Salto, F. Santoyo-González, J. M. García Fernández, *Org. Biomol. Chem.* **2009**, *7*, 2681-2684.
[4] C. Tschierske, *Prog. Polym. Sci.* **1996**, *21*, 775–852.
[5] J.-M. Lehn, *Angew. Chem. Int. Ed.* **1990**, *29*, 1304-1319.
[6] P. Metrangolo, F. Meyer, T. Pilati, G. Resnati and G. Terraneo, *Angew. Chem. Int. Ed.* **2008**, *47*, 6114–6127.
[7] C.-C. Ling, R. Darcy and W. Risse, *Chem. Commun.* **1993**, 438-440.
[8] L. Chen, T.-H. Hu, H.-L. Xie and H.-L. Zhang, *J. Polym. Sci. Pol. Chem.* **2010**, *48*, 2838-2845.
[9] F. Yang, Y. Zhang, H. Guo, *New J. Chem.* **2013**, *37*, 2275–2279.
[10] S. Ward, O. Calderon, P. Zhang, M. Sobchuk, S. N. Keller, V. Williams and C.-C. Ling, *J. Mater. Chem. C* **2014**, *2*, 4928-4936.
[11] J. Terao, S. Tsuda, Y. Tanaka, K. Okoshi, T. Fujihara, Y. Tsuji, N. Kambe, *J. Am. Chem. Soc.* **2009**, *131*, 16004–16005.
[12] P. Zhang, C. Ling, A. Coleman, H. Parrot-Lopez, H. Galons, *Tetrahedron Lett.* **1991**, *32*, 2769–2770.
[13] P. Zhang, H. Parrot-Lopez, P. Tchoreloff, A. Baszkin, C. Ling, C. Derango, A. Coleman, *J. Phys. Org. Chem.* **1992**, *5*, 518–528.
[14] H. Parrot-Lopez, C. Ling, P. Zhang, A. Baszkin, G. Albrecht, C. Derango, A. Coleman, *J. Am. Chem. Soc.* **1992**, *114*, 5479–5480.
[15] A. Méndez-Ardoy, N. Guilloteau, C. Di Giorgio, P. Vierling, F. Santoyo-González, C. Ortiz Mellet, J. M. García Fernández, *J. Org. Chem.* **2011**, *76*, 5882–5894.
[16] A. Mazzaglia, R. Donohue, B. J. Ravoo, R. Darcy, *Eur. J. Org. Chem.* **2001**, 1715–1721.
[17] A. Mazzaglia, A. Valerio, N. Micali, V. Villari, F. Quaglia, M. A. Castriciano, L. M. Scolaro, M. Giuffrè, G. Siracusano, M. T. Sciortino, *Chem. Commun.* **2011**, *47*, 9140-9142.
[18] T. Kato, N. Mizoshita and K. Kishimoto, *Angew. Chem. Int. Ed.* **2006**, *45*, 38-68.

[19] V. G. Avakyan, V. B. Nazarov, M. V. Alfimov, A. A. Bagatur'yants and N. I. Voronezheva, *Russ. Chem. Bull. Int. Ed.* **2001**, *50*, 206-216.
[20] R. Huisgen, *Proc. Chem. Soc.* **1961**, 357-396.
[21] H. C. Kolb, M. G. Finn and K. B. Sharpless, *Angew. Chem. Int. Ed.* **2001**, *40*, 2004–2021.
[22] S. Ward and C.-C. Ling, *Eur. J. Org. Chem.* **2011**, 4853-4861.
[23] J. Gu, T. Chen, P. Zhang and C.-C. Ling, *Eur. J. Org. Chem.* **2014**, 5793-5805.
[24] J. Gu, T. Chen, Q. Wang and C.-C. Ling, *Carbohydr. Res.* **2015**, *410*, 36-46.
[25] S. Ballut, D. Naud-Martin, B. Loock, P. Maillard, *J. Org. Chem.* **2011**, *76*, 2010 – 2028.
[26] P. Fugedi, *Carbohydr. Res.* **1989**, *192*, 366–369.
[27] A. W. Coleman, P. Zhang, C.-C. Ling and H. Parrot-Lopez, *Carbohydr. Res.* **1992**, *224*, 307-309.
[28] C. Lavigueur, E. Foster and V. Williams, *J. Appl. Crystallogr.* **2008**, *41*, 214-216.
[29] K. Lindner and W. Saenger, *Carbohydr. Res.* **1982**, *99*, 103–115

Entry for the Table of Contents (Please choose one layout)

Layout 1:

FULL PAPER

A novel concept to design amphiphilic cyclodextrin (CD)-based liquid crystals is reported. The new CD derivatives bear O-acetylated oligoethylene glycol chains at the secondary face and thioalkyl groups at the primary face and self-assemble into highly ordered smectic liquid crystal phases with much improved properties via the weaker dipole-dipole interactions.

*Pier-Luc Champagne,[a] David Ester,[b] Sandra Ward,[c] Vance E. Williams[b] and Chang-Chun Ling[a]**

First Family of Amphiphilic Cyclodextrin Liquid Crystals Drived By Dipole-Dipole Interactions

Layout 2:

FULL PAPER

((Insert TOC Graphic here; max. width: 11.5 cm; max. height: 2.5 cm))

Page No. – Page No.

Text for Table of Contents